Kinetic and isotherm studies of adsorption processes in the removal of reactive dyes from aqueous solutions

IOP ebooks™

Bringing you innovative digital publishing with leading voices to create your essential collection of books in STEM research.

Start exploring the collection - download the first chapter of every title for free.

Kinetic and isotherm studies of adsorption processes in the removal of reactive dyes from aqueous solutions

A Syafiuddin[1], T Hadibarata[2], A Yuniarto[3], A C Tay[2], S K Ali[4], T Hidayat[5]

[1] Department of Water and Environmental Engineering, Universiti Teknologi Malaysia, 81310 UTM Skudai, Johor, Malaysia

[2] Department of Environmental Engineering, Curtin University, Malaysia, 98009 Miri Sarawak, Malaysia

[3] Department of Environmental Engineering, Faculty of Civil, Environmental and Geo Engineering, Institut Teknologi Sepuluh Nopember, 60111 Surabaya, Indonesia

[4] Department of Medical Microbiology and Parasitology, Universiti Putra Malaysia, 43400 Serdang, Malaysia

[5] Biology Education Department, Universitas Pendidikan Indonesia, Jl Dr. Setiabudi No. 229, Bandung, Indonesia

[a]Corresponding author: hadibarata@curtin.edu.my

Abstract. This work was aimed to evaluate the capability of activated carbon prepared from Bamboo (Bambusa bambos) stems (BS) to remove two reactive dyes, which are Malachite Green G (MGG) and Reactive Red 2 (RR2) from aqueous media. The presently proposed activated carbon was prepared using the chemical activation. The activated carbon was also characterized by means of the Fourier Transform Infrared Spectrometry and Field Emission Scanning Electron Microscopy. To investigate the kinetic and isotherm characteristics, the adsorption tests were carried out in a batch experiment and then several mathematical models were employed for describing the experimental data. The present work has found that the proposed activated carbon was capable to remove the dyes with an adsorption capacity of 3.80 mg/g and 2.22 mg/g of MGG and RR2, respectively, for 60 min. The equilibrium data were described well by Freundlich isotherm model for both MGG and RR2. The pseudo-second-order model performed well the experimental kinetic data.

1. Introduction

In recent years, industrialization has left its impression on the environmental society. Textile industries especially use dyes to colour their products and thus produce wastewater containing the dyes. The contaminated water may affect human who use for living purposes such as washing, bathing, and most importantly for drinking purposes. Moreover, the presence of the dyes in the water environment affects the photosynthetic activity in aquatic life by reducing light penetration and may also be toxic to aquatic biota because of the presence of metals and chlorides [1]. Malachite green G (MGG) is one of the triarylmethane dyes which are closely related to malachite green. It is also known as ethyl green,

emerald green, benzaldehyde green, solid green JJO, diamond green G, aniline green, and fast green J Green is a dye indicator that changes from yellow to green at pH 0.0 to 2.6. It can be also used as a topical antiseptic and as a selective bacteriostatic agent in culture media. Reactive red 2 (RR2) is a brand of fiber reactive dyes. The aforementioned dyes have complex chemical structure, high molecular weight, and high solubility in water.

Several methods have been implemented to remove pollutant from the water solution, [2,3,4,5,6,7,8,9]. Among these, the adsorption process is recently preferred by researchers. Adsorption is claimed as the most potential method for removing dyes from aqueous solutions [10]. Adsorption of dyes onto activated carbon was considered as an efficient method to control organic pollutants in water. However, high cost of commercial activated carbon is one of constraints so that researchers pay attention to identify an alternative low-cost precursor for the preparation of activated carbon.

Preparation of activated carbon from various agricultural wastes for treatment of wastewater has been widely explored. Due to its large surface area, activated carbon is widely used for recent years. Activated carbon has a high adsorption capability because of its high internal surface area and porosity gained from the carbonization process. The development of pore structure is due to the presence of an activating agent and perfect carbonization condition. By activation methods including dry and wet oxidizing agents, the surface oxygen functional groups can be easily introduced to the carbon. The dry oxidation method involves the reaction at high temperature. Wet oxidation comprises the reaction between the carbon surface and solution of oxidizing agents by employing several activating agents such as zinc chloride ($ZnCl_2$), phosphoric acid (H_3PO_4), nitric acid (HNO_3), potassium permanganate ($KMnO_4$), hydrogen peroxide (H_2O_2), potassium hydroxide (KOH), and ammonia sulphate ($(NH_4)_2SO_8$).

Recently, exploration of natural resources to produce advanced materials is widely carried out [11,12,13,14]. Bamboo is fast growing natural resource and is readily available which offers great potential applications. Bamboo generally contains cellulose, hemicellulose, and lignin. By having cellulose, hemicellulose and lignin, these make agricultural wastes as an effective adsorbent for the removal of dyes due to the presence of functional groups for example carboxyl, hydroxyl, phenols, and methoxy. These functional groups play an important role in the binding pollutants [15]. Bamboo-based activated carbons have been intensively used as an adsorbent for effective removal of dyes. For instance, adsorption of methylene blue on the bamboo-based activated carbon using microwave radiation has been reported [16]. Their study found that the enhancement of the adsorption of methylene blue on the proposed activated carbon was controlled by the enlargement of the micropores. By employing different procedure, an activated carbon prepared by the physiochemical activation with potassium hydroxide and carbon dioxide was also successful for removal of methylene blue. Alternatively, the adsorption of acid dyes such as acid Yellow 117 and acid Blue 25 on the modified activated carbon has been also ratified [17]. Their study found that the adsorption acid dyes on the modified activated carbon was affected by surface area and porosity of the activated carbon [17]. Moreover, bamboo-based activated carbons were also reported as adsorbent for removal of formaldehyde [18], ciprofloxacin [19], blend Yellow D-3RNL [20].

Therefore, this study aims to evaluate the capability of the activated carbon prepared from the bamboo stems (BS) to remove other dyes such as Malachite Green G (MGG) and Reactive Red 2 (RR2) from aqueous media. Although activated carbon from bamboo has been widely used to remove dyes, findings of this study provide additional knowledge the performance of bamboo to remove other dyes, which has also possible different in terms of mechanism process. Thus, surface and functional group characterizations of the adsorbents were investigated using Field Emission Scanning Electron Microscopy (FESEM) and Fourier Transform Infrared Spectroscopy (FTIR), respectively.

2. Materials and method

2.1. Materials
Bamboo stem (BS) used in this experiment was obtained from surrounding area of the Universiti Teknologi Malaysia (UTM), Johor Bahru, Malaysia. BS were then used to produce activated carbon.
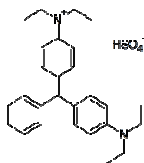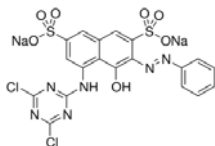
Zinc chloride was supplied by Qrec, Malaysia. MGG and RR2 were supplied by Aldrich, USA. Other chemicals used were analytical reagent grade.

2.2. Stock solution preparation and Activated carbon production
Stock solutions of MGG and RR2 were prepared by diluting 30 mg of MGG and RR2 powder with 1000 mL of the distilled water. The series of 5, 10, 15, 20, 25 and 30 mg/L of MGG and RR2 standard solution were prepared from this stock solution. Table 1 shows the physical-chemical characteristics of MGG and RR2.

Raw BS were washed for several times using tap water to remove any impurities and then dried under ambient atmosphere for 24 h. Next, BS were entered into an oven at 105°C overnight. The dried bamboo stems were impregnated with 10% $ZnCl_2$ solution for 24 h. The solution was then decanted off and the impregnated bamboo stems were dried in an oven at 105°C before carbonized in a furnace. Carbonization was performed in a horizontal furnace, under nitrogen gas at 500°C for 1 h; the N_2 flow rate was 2.5 L/min. The activated carbon was washed with the distilled water until pH of the washed water becomes neutral (±7). It was then dried at 105°C for 3 h, grounded (1 mm in an average of size from sieving analysis), and stored in a container at room temperature.

Table 1. Physical and chemical characteristics of MGG and RR2

Dye	MGG	RR2
Chemical structure		
Synonym	Fast green J	Procion Red
Appearance	Dark green	Dark red
Physical state	Crystalline powder	Powder
Solubility	100 g/L a 20 °C	Yes
Melting point	210 °C	>300°C
Molecular weight	482.63 g mol^{-1}	615.34 g mol^{-1}
Molecular formula		
Max. wavelength	$C_{27}H_{34}N_2O_4S$	$C_{19}H_{10}Cl_2 N_6Na_2O_7S_2$
	623 nm	538 nm

2.3. Adsorption experiment
Adsorption tests were carried out in a batch experiment. The batch experiments were performed in 100 ml conical flasks by introducing 50 mL of MGG and RR2 solution using several concentrations. Activated carbon of 0.3 g was added to each flask. The flasks were shaken at 150 rpm using a mechanical shaker at room temperature (±27°C). The speed was kept constant throughout the experiment to ensure equal mixing. The adsorption kinetic was evaluated over contact time from 10 to 100 min. The effect of MGG and RR2 concentration were studied using concentration ranging from 5 to 30 mg/L. The influence of the activated carbon loading on MGG and RR2 adsorption were investigated over the adsorbent dosage of 0.1 to 0.6 g. The experiment was performed in duplicate. The flask containing the sample was removed from the shaker at the predetermined time and the sample was filtered using the Advantec filter paper. The color removal (%) and the adsorption capacity, q_e (mg/g), were calculated by the following formula:

$$\text{Color removal (\%)} = \frac{C_o - C_e}{C_o} x100 \tag{1}$$

$$\text{Adsorption capacity} = \frac{C_o - C_e}{X} xV \tag{2}$$

where C_o and C_e are the liquid-phase concentrations of MGG and RR2 at initial and equilibrium (mg/L), V is the volume of MGG and RR2 solution (L), and X is the mass of adsorbent (g) used [21].

2.4. Isotherm and kinetic studies

The Langmuir equation is applicable to homogenous sorption whereas Freundlich is applicable to heterogeneous sorption [21]. The Langmuir adsorption model is based on the assumption that the maximum adsorption corresponds to a saturated monolayer of solute molecules on the adsorbent surface. The Langmuir adsorption isotherm has been successfully used to explain the adsorption of basic dyes from aqueous solutions [22,23]. Langmuir model is mathematically expressed as:

$$\text{Langmuir equation, } q = \frac{K_L q_m C_e}{1 + K_L C_e} \tag{3}$$

where C_e (mg/L) is the concentration of MGG and RR2 solution at equilibrium, q (mg/g) is the amount of sorbed MGG and RR2 at equilibrium, q_m is the maximum sorption capacity, and K_L is the Langmuir constant.

$$\text{Freundlich equation, } q = K_f C_e^{1/n} \tag{4}$$

where C_e (mg/L) is the concentration of MGG and RR2 solution at equilibrium, q (mg/g) is the amount of sorbed MGG and RR2 at equilibrium, K_F and n are the Freundlich constants.

Evaluation of the reaction kinetics is important for determining the rate of adsorbate uptake during the adsorption. The MGG and RR2 sorption kinetics were investigated by examining the influence of contact time on MGG and RR2 removal for 100 min. Aqueous samples were taken at interval time and the concentrations of residual MGG and RR2 were measured. The commonly used adsorption kinetic models are the Pseudo-first-order and Pseudo-second-order. The best-fit model was selected based on R^2 values. The kinetics data for MGG and RR2 adsorption were treated with the following Pseudo-first-order and Pseudo-second-order models:

$$\text{Pseudo-first-order, } q(t) = q_e(1 - \exp(-k_1 t)) \tag{5}$$

$$\text{Pseudo-second-order, } q(t) = \frac{k_2 q_e^2 t}{1 + q_e k_2 t}$$
$$\tag{6}$$

where q_e and $q(t)$ (mg/g) respectively refer to the amount of MGG and RR2 adsorbed at equilibrium and at time t (min); k_1 is the rate constant of pseudo-first-order, and k_2 is the rate constant of pseudo-second-order.

2.5. Characterizations

The functional group on the surface of the raw bamboo stems and bamboo-activated carbons were analyzed using the Fourier Transform Infrared Spectrometry (FTIR) (Spectrum one, Perkin Elmer, USA). The activated carbon was mixed with KBr powder at 100:1 weight ratio then pressed using hydraulic press into KBr pellet. The spectra were scanned in the wavenumber ranging from 4000 to 400 cm^{-1}. The surface morphology of the raw bamboo stems, BS-activated carbon, BS-activated carbon after adsorption process for both MGG and RR2 were investigated using the Field Emission Scanning Electron Microscope (FESEM, JEOL 6335F-SEM, Japan), and elementary analyses were performed simultaneously using EDX spectrometer. Pollutant concentration of the sample was measured by acquisition of the UV/Vis spectrophotometer (NANOCOLOR® VIS, Macherey-Nagel, Germany) at the maximum wavelength of 623 nm for MGG and 534 nm for RR2.

3. Results and discussion

3.1. Characterization of adsorbents

BS analyzed by FTIR spectroscopy to determine the surface functional groups responsible for MGG and RR2 uptakes during the adsorption process. Figure 1 shows the FTIR spectra of raw BS and BS-activated carbon. Raw BS showed the broad peak at 3410.51 cm^{-1}, which is assigned to the stretching vibration of the O-H hydroxyl group. The absorption peak at 2924.46 cm^{-1} is attributed to C-H stretching vibration of the alkane group. The small peaks at 1700-1730 cm^{-1} are attributed to C=O and C-O stretching of carbonyl, esters and carboxylic acid. The peak at 1616.35 cm^{-1} is assigned to amine group. The peaks between 1260 and 1000cm^{-1} are ascribed to either C-O stretching and Si-O as a yield of silica containing minerals [24].
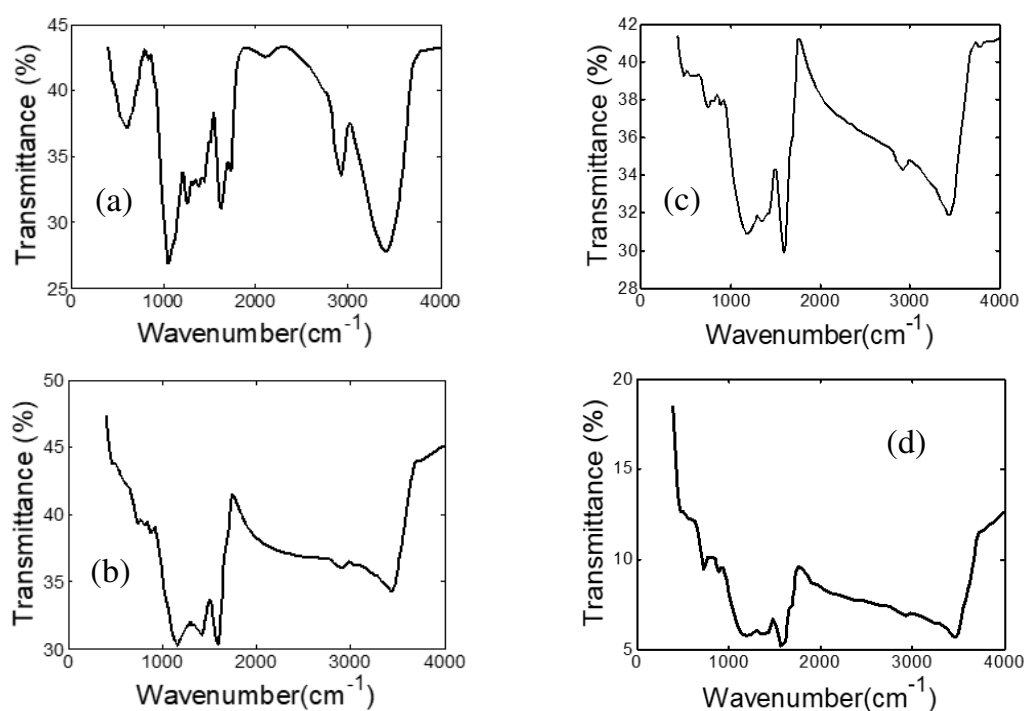

Figure 1. (a) FTIR spectra of raw BS, (c) BS-activated carbon, (c) BS-activated carbon after adsorption of RR2 and (d) BS-activated carbon after adsorption of MGG

3.2. Batch studies

After raw BS was converted to activated carbon, the strong bond was observed at 1588.27cm^{-1}, which is possibly due to the intense stretching of conjugated C=C in aromatic ring or oxygen-aromatic bonding in aromatic ether. At 3437.31cm^{-1}, which is attributed to the O-H stretching vibration was weaker than O-H stretching. This is due to the loss of hydroxyl groups and elimination of volatile molecules from raw BS. The peak at 1418.02cm^{-1} is ascribed to C-C stretching. The intensity of band located at 1700-1730 cm^{-1} ascribed to C=O stretching was also weakened and the reduction of complex band at 1260-1000 cm^{-1} was observed which include the reduction of carboxylic acids, alcohol, and ester (Figure 1).

FESEM analysis of the surface morphology of the BS before and after carbonization was depicted in Figure 2. All the images were observed at a magnification of ×1000. The surface of the raw BS was rough with a very few pores. After treatment with ZnCl$_2$, more pores were developed on the surface of

BS-activated carbon. The FESEM analysis of the surface of BS-activated carbon clearly showed that BS-activated carbon contained many small cavities with an average size of 3-5μm. The development of porosity of BS-activated carbon was influenced by burning temperature of the pyrolysis RR2ocess and the activation of Zinc Chloride ($ZnCl_2$). $ZnCl_2$ acts as dehydrating agent which induces the charring and restricts the formation of tar [25]. The surface morphology of BS-activated carbon after adsorption with MGG and RR2 are indicated by a lot of pores with larger in size which aided during the adsorption process. In order to develop BS-activated carbon, BS was carbonized with $ZnCl_2$ in one-step carbonization Process. The use of $ZnCl_2$ can develop micro pores and create active sites on BS-activated carbon surfaces [25].
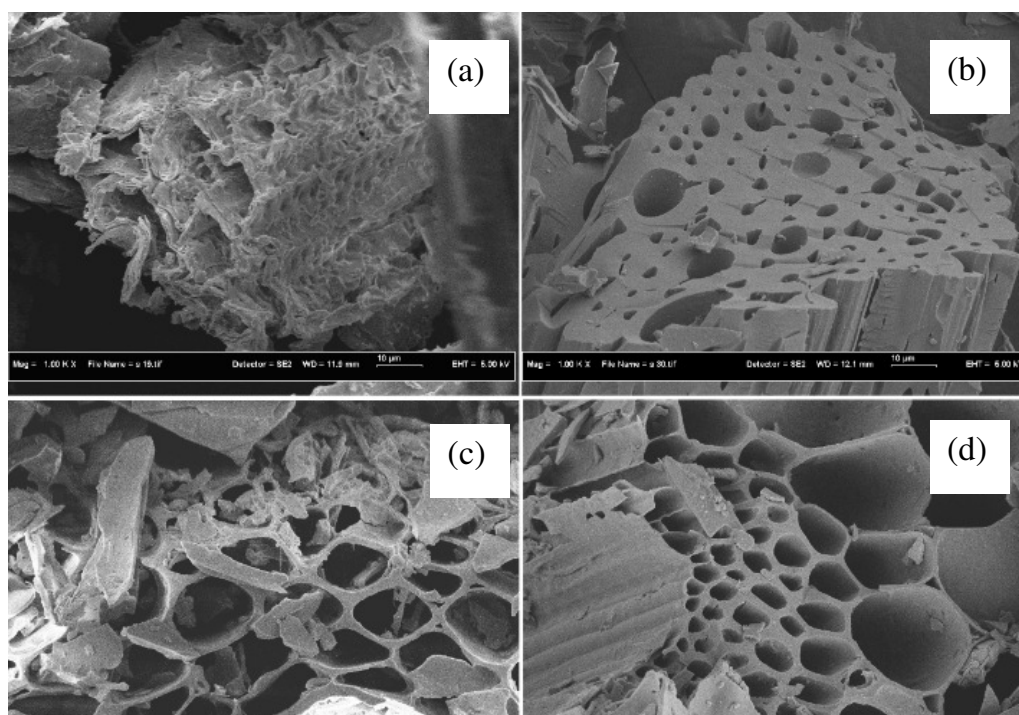

Figure 2. (a) Morphology structure of raw BS, (b) BS-activated carbon, (c) after adsorption of MGG, and (d) after adsorption of RR2.

Table 2 shows the percentage of removal and adsorption capacity for MGG and RR2. For MGG, the adsorption increased with increasing contact time of MGG with the activated carbon. It can be seen that the increasing contact time tends to increase percent removal and adsorption capacity. Optimum adsorption equilibrium was achieved at 60 min, with a percentage of 82.25 % and adsorption capacity of 3.80 mg/g. The adsorption process was initiated with rapid adsorption until it reached equilibrium at 60 min, due to readily accessible sites. RR2 also achieved equilibrium at min of 60. Percentage removal of RR2 and adsorption capacity also increased against time. The adsorption RR2 started with rapid adsorption within the first 40 min, followed by slower adsorption within the period of 40-60 min. In the slower adsorption, the accessible sites are decreased. Finally, a plateau was reached after 60 min, indicating the activated carbon was saturated. The percentage removal and adsorption capacity of RR2 at equilibrium were 44.39 % and 2.22 mg/g, respectively.

The adsorption capacities obtained in this work are in line with those of previous studies. For instance, an activated carbon prepared from bamboo for the adsorption of Red dye has adsorption capacities in the range of 1.28 to 2.46 mg/g [26]. Alternatively, adsorption capacity of 1.38 mg/g was also found when the bamboo-base activated carbon was employed for the adsorption of direct blend

Yellow D-3RN [20]. For both MGG and RR2, after the optimal adsorption achieved, for 60 min onwards, the percentage of removal and adsorption capacity were slightly decreased. This might be due to the release of some MGG and RR2 molecules from adsorbent surface. Dyes achieved equilibrium faster in just few minutes compared to BPA, which the removal of BPA with sugi chip and sawdust [27].

MGG and RR2 concentration were varied from 5-30 mg/L. Percentage removal for both MGG and RR2 decreased with concentration. MGG recorded the highest percentage of removal 95.68 % which the dropped to 80.07 %. RR2 percent removal decreased from 53.61 % which then dropped to 40.43 %. On the other hand, adsorption capacity for both dyes increased with concentration. Adsorption capacity of MGG increased from 0.98 to 3.70 mg/g whereas RR2 from 0.43 to 2.02 mg/g. With increasing of initial concentration of MGG and RR2, the driving force of mass transfer became more dominant, thereby enhancing the driving force to get over mass transfer resistance between MGG and RR2 in solution and activated carbon, resulting in higher adsorption capacity. This phenomenon was also observed in other study when methylene blue concentration was increased from 50 to 500 mg/L, and initial bisphenol A concentration was increased from 60-100 mg/L [23,28]. At higher initial concentration, the ratio of adsorbate to adsorbent is low thus decreasing the removal percentage [23,28].

Table 2. Effect of contact time on MGG and RR2

Time (min)	MGG Removal (%)	RR2 Removal (%)
10	77.76	26.24
20	78.39	31.02
30	79.64	36.80
40	80.57	41.91
50	81.46	43.07
60	82.25	44.39
70	82.22	43.89
80	82.15	43.23
90	82.09	42.90
100	81.99	42.41

The effect of adsorbent dosage on the adsorption of MGG and RR2 was evaluated by varying of activated carbon concentration from 0.1 to 0.6 g. The results show that the adsorption efficiency is dependent on the amount of activated carbon added; increasing the activated carbon loading may increase the percentage removal of MGG and RR2 but decrease the adsorption capacity. The maximum removal for MGG and RR2 were at 0.4 g, further loading of adsorbent did not give any considerable change of removal. The adsorption capacity for MGG at the loading of 0.4g was 2.84 mg/g, which is less than achieved with an adsorbent loading of 0.3 g (3.79 mg/g). RR2 recorded 1.62 mg/g at 0.4g of loading and 2.15 mg/g at 0.3g. Therefore, a minimum loading of 0.3g of adsorbent was more effective for removal of MGG and RR2 from a 50 mL of dye solution of 30 mg/L MGG and RR2. The similar trend was also observed by previous studies that the decrease of adsorption capacity was probably caused by the split in the concentration gradient between adsorbates in the solution and in the adsorbent surface [29].

3.3. Adsorption isotherm

Figure 3 shows the performance of the presently employed isotherm models compared to the experimental data. This study found that the adsorption of MGG on the activated carbon can be described well when Freundlich isotherm model was employed with R^2 value of 0.99. Similar finding was also found when RR2 was used as a pollutant model. It was found that Freundlich isotherm model

performed well compared to Langmuir isotherm model. It is then ratified that Freundlich model provided a better fit to explain the adsorption of MGG and RR2 on the presently proposed activated carbon. Freundlich isotherm considers the BS-activated carbon multilayer adsorption with a heterogeneous energetic distribution of active sites, accompanied by interactions between adsorbed molecules.
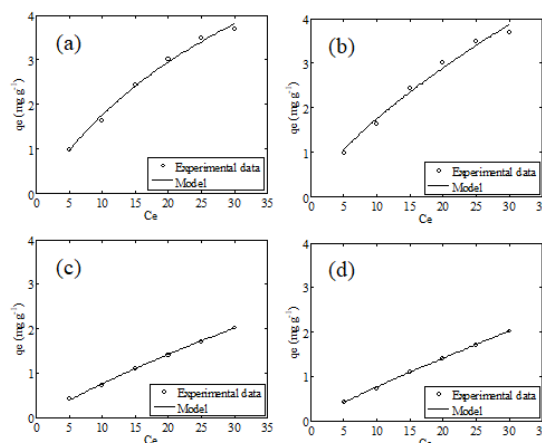

Figure 3. (a) Langmuir model for the adsorption of MGG, (b) Freundlich model for the adsorption of MGG, (c) Langmuir model for the adsorption of RR2, and (d) Freundlich model for the adsorption of RR2.

The objective of this adsorption isotherm was to relate the adsorbate concentration in the bulk and the adsorbed amount at the interface and gave a complete understanding on the nature of interaction. The parameters obtained from different models provided relevant information on the surface properties of the adsorbent and its affinity to the adsorbate. It indicated the distribution of MGG and RR2 in the equilibrium phase.

3.4. Adsorption kinetic
Figure 4 presents the performance of all employed kinetic models compared to the experimental data. Iit was found that the Pseudo-second order model performed well compared to the Pseudo-first-order model. This study found that R^2 for Pseudo-second order model was 0.81 and 0.93 for adsorption of MGG and RR2, respectively. Hence, it was concluded that the adsorption of MGG and RR2 can be better explained by the Pseudo-second-order model and the process is chemisorption (Nandi et al. 2008). Pseudo-second-order kinetic was also reported to perform well for adsorption of methylene blue onto perlite and the adsorption of Cr (IV) onto olive bagasse-derived activated carbon [30].
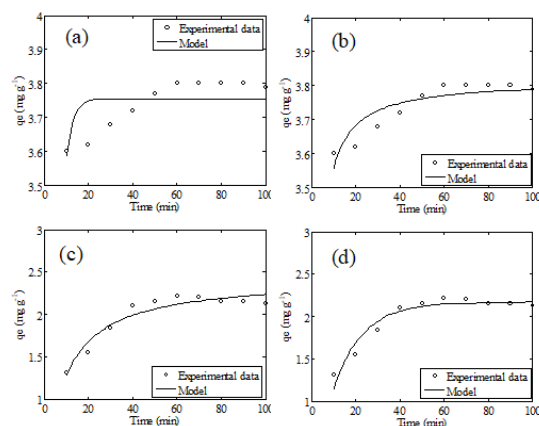
Figure 4. (a) Pseudo-first-order model for the adsorption of MGG, (b) Pseudo-second-order model for the adsorption of MGG, (c) Pseudo-first-order model for the adsorption of RR2, and (d) Pseudo-second-order model for the adsorption of RR2.

4. Conclusion

Activated carbon produced from BS activated using zinc chloride at a temperature of 500°C was investigated in this work. MGG and RR2 have been successfully removed from aqueous media. Up to 82.25 % of the percentage of removal and adsorption capacity of 3.80 mg/g with adsorption time of 60 min were found in this work. Meanwhile at the same adsorption time, RR2 only was removed by achieving the percent of removal of 44.39 % and 2.22 mg/g of adsorption capacity which is less effective than MGG. For both dyes, the isotherm data showed better correlation with the Freundlich isotherm model. In kinetic model, MGG and RR2 can be described well using the Pseudo-second-order model compared to the Pseudo-first-order model. From this work, it was ratified that MGG was found to be favourable, and BS-activated carbon became a prospective low-cost compared to commercial adsorbents.

Acknowledgements

References

[1]   Tahir U, Yasmin A and Khan U H 2016 *J. King Saud Univ. Sci.* **28** 119-130
[2]   Nor N M, Hadibarata T, Zubir M M F A, Lazim Z M, Adnan L A and Fulazzaky M A 2015 *Bioprocess Biosyst. Eng.* **38** 2167-2175
[3]   Hadibarata T and Kristanti R A 2014 *Fungal Biol.* **118** 222-227
[4]   Syafiuddin A, Salmiati, Salim M R, Kueh A B H, Hadibarata T and Nur H 2017 *J. Chin. Chem. Soc.* **64** 732-756
[5]   Hadibarata T, Yusoff A R M, Aris A, Salmiati, Hidayat T and Kristanti R A 2012 *Water Air Soil Pollut.* **223** 1045-1054
[6]   Kristanti R A, Kamisan M K A and Hadibarata T 2016 *Water Air Soil Pollut.* **227** 1-7
[7]   Rubiyatno, Hadibarata T, Yanti N, Seng B 2012 *J. Enviro. Sci. Technol.* **5** 430-440
[8]   Khudhair A B, Hadibarata T, Kamyab H, Kristanti R A 2017 *Bioproc. Biosys. Eng.* **40** 1411-1418
[9]   Kristanti R A, Kambe M, Hadibarata T, Toyama T, Tanaka Y, Mori K 2012 *Environ. Sci. Pollut. Res.* **19** 1852-1858
[10]   Gupta V K and Suhas 2009 *J. Environ. Manage.* **90** 2313-2342

[11]   Syafiuddin A, Salmiati, Hadibarata T, Salim M R, Kueh A B H and Sari A A 2017 *Bioprocess Biosyst. Eng.* **40** 1349-1361

[12]   Nikmatin S, Syafiuddin A, Hong Kueh A B and Maddu A 2017 *J. App. Res. Technol.* **15** 386-395

[13]   Syafiuddin A, Salmiati, Hadibarata T, Kueh A B H and Salim M R 2018 *Nanomaterials* **8** 1-17

[14]   Hadibarata T, Syafiuddin A, Al-Dhabaan F A, Elshikh M S and Rubiyatno 2018 *Bioprocess Biosyst. Eng.* **41** 621-632

[15]   Lin D and Xing B 2008 *Environ. Sci. Technol.* **42** 7254-7259

[16]   Liu Q-S, Zheng T, Li N, Wang P and Abulikemu G 2010 *Appl. Surf. Sci.* **256** 3309-3315

[17]   Chan L S, Cheung W H, Allen S J and McKay G 2009 *Sep. Purif. Technol.* **67** 166-172

[18]   Rengga W D P, Chafidz A, Sudibandriyo M, Nasikin M and Abasaeed A E 2017 *J. Env. Chem. Eng.* **5** 1657-1665

[19]   Wang Y X, Ngo H H and Guo W S 2015 *Sci. Total Environ.* **533** 32-39

[20]   Wang L 2013 *Desalin. Water Treat.* **51** 5792-5804

[21]   Doğan M, Abak H and Alkan M 2008 *Water Air Soil Pollut.* **192** 141-153

[22]   Hameed B H and Rahman A A 2008 *J. Hazard. Mater.* **160** 576-581

[23]   Tan I A W, Ahmad A L and Hameed B H 2008 *J. Hazard. Mater.* **154** 337-346

[24]   Al-Qodah Z and Shawabkah R 2009 *Braz J Chem Eng* **26** 127-136

[25]   Hayashi J i, Kazehaya A, Muroyama K and Watkinson A P 2000 *Carbon* **38** 1873-1878

[26]   Wang L 2013 *Environ. Sci. Pollut. Res.* **20** 4635-4646

[27]   Nakanishi A, Tamai M, Kawasaki N, Nakamura T and Tanada S 2002 *J. Colloid Interface Sci.* **252** 393-396

[28]   Tsai W-T, Lai C-W and Su T-Y 2006 *J. Hazard. Mater.* **134** 169-175

[29]   Han X, Wang W and Ma X 2011 *Chem. Eng. J.* **171** 1-8

[30]   Demiral H, Demiral İ, Tümsek F and Karabacakoğlu B 2008 *Chem. Eng. J.* **144** 188-196